Sense–Analyze–Respond–Actuate (SARA) Paradigm: Proof of Concept System Spanning Nanoscale and Macroscale Actuation for Detection of *Escherichia coli* in Aqueous Media

Cassie A. Giacobassi [1], Daniela A. Oliveira [1], Cicero C. Pola [2], Dong Xiang[3,4], Yifan Tang[3], Shoumen Palit Austin Datta [3,5,6,7], Eric S. McLamore [3,*] and Carmen L. Gomes [2,*]

[1] Department of Biological and Agricultural Engineering, Texas A&M University, College Station, TX, 77843, USA; c.giacobassi@gmail.com (C.A.G.); daoliveira@tamu.edu (D.A.O.)

[2] Department of Mechanical Engineering, Iowa State University, Ames, IA, 50011, USA; cicerocp@iastate.edu (C.C.P)

[3] Agricultural and Biological Engineering, Institute of Food and Agricultural Sciences, University of Florida, Gainesville, FL, 32611, USA; xiangdong@ufl.edu (D.X.); tang.yifan@ufl.edu (Y.T.); shoumen@mit.edu (S.P.A.D.)

[4] School of Integrative Sciences and Engineering, Centre for Life Sciences, National University Singapore, Singapore, 119077, Singapore

[5] MIT Auto-ID Labs, Department of Mechanical Engineering, Massachusetts Institute of Technology, Cambridge, MA, 02139, USA

[6] MDPnP Labs, Biomedical Engineering Program, Department of Anesthesiology, Massachusetts General Hospital, Harvard Medical School, Cambridge, MA 02139, USA

[7] NSF Center for Robots and Sensors for Human Well-Being (RoSeHuB), Collaborative Robotics Lab, 193 Knoy Hall, Purdue University, West Lafayette, IN 47907, USA

* Correspondence: emclamore@ufl.edu (E.S.M); carmen@iastate.edu (C.L.G); Tel.: +1-352-294-6703 (E.S.M); +1-515-294-1138 (C.L.G)

Time course for SARA system
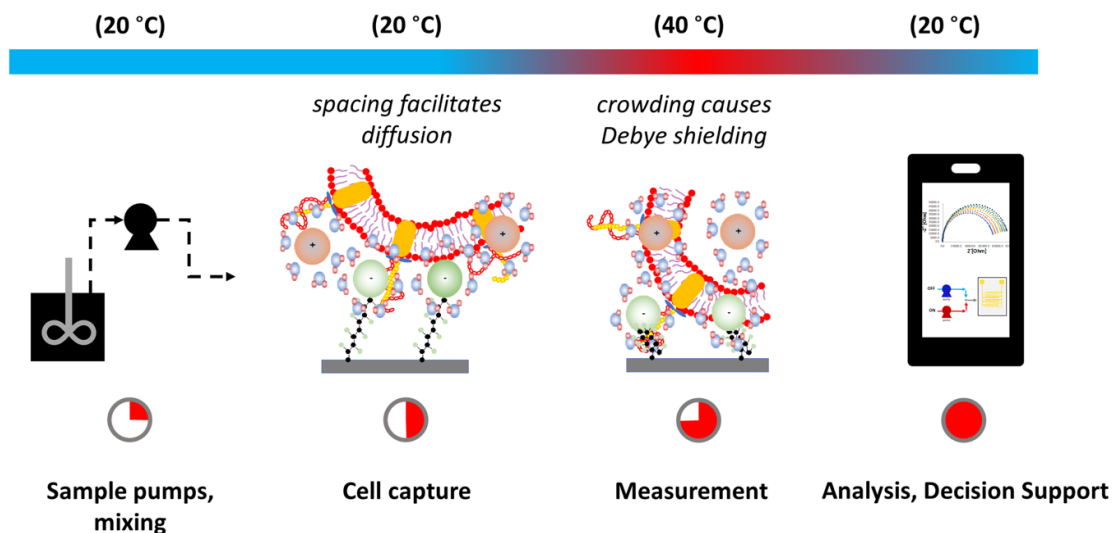
Figure S1. Time course of SARA testing system. Sample pumps provide mixing, sampling, and temperature control. Cell capture on the biosensor surface occurs at 20°C when the nanobrush is extended. The spacing of materials near the electrode surface facilitates diffusion of redox probe and electrolyte. During measurement, the increase of temperature causes nanobrush collapse, which induces crowding near the electrode surface and a change in signal due to Debye shielding. Upon return to 20°C a third impedance measurement is taken and the data are analyzed to provide on-site decision support regarding fecal contamination. The process takes approximately 40 min.

Screen printed carbon (SPC) electrode surface activation

SPC electrode surface activation was performed by cyclic voltammetry in a three-electrode setup using Ag/AgCl as reference electrode and a Pt-wire as counter electrode. The SPC electrodes were dipped in 10 mL of 0.5 M sulfuric acid solution and 10 scans were performed from -1.5 to 1.5 V.

Functionalized SPC electrode storage

After functionalization, SPC electrodes were freeze-dried according to Soares et al. [1]. Shortly, 100 μL of 1x PBS was added to the working area of SPC electrode and they were stored at –20 °C for 12 h. Then, the frozen biosensors were freeze-dried for 24 h at –50 °C and 0.130 mbar using a FreeZone 4.5 L Freeze Dryer System (Labconco, Kansas City, MO, USA). Later, the freeze-dried biosensors were stored at –20 °C until shipping from Iowa State University to the University of Florida for hydroponic experiments. The influence of freeze-drying process over the electrochemical properties of SPC biosensors were evaluated by CV.

ConA functionalized SPC were evaluated by CV before and after freeze-drying process. No significant change in peak potential ($p > 0.05$) or peak current ($p > 0.05$) were observed for the freeze-dried electrodes (Figure S2).
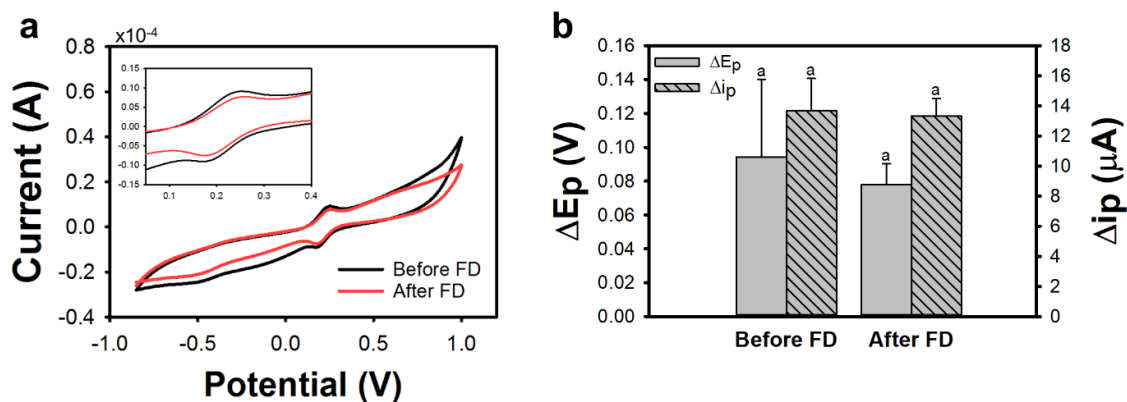
Figure S2. (**a**) Cyclic voltammograms of the SPC functionalized electrodes before and after the freeze-drying process. (**b**) Change in peak potential (ΔE_P, volts) and change in peak current (Δi_P, μA) before and after freeze-drying. Error bars denote standard deviation (n = 3). Different letters indicate significant difference using t-test at significance level of 5%.

Hydroponic system

SARA sampling process flow
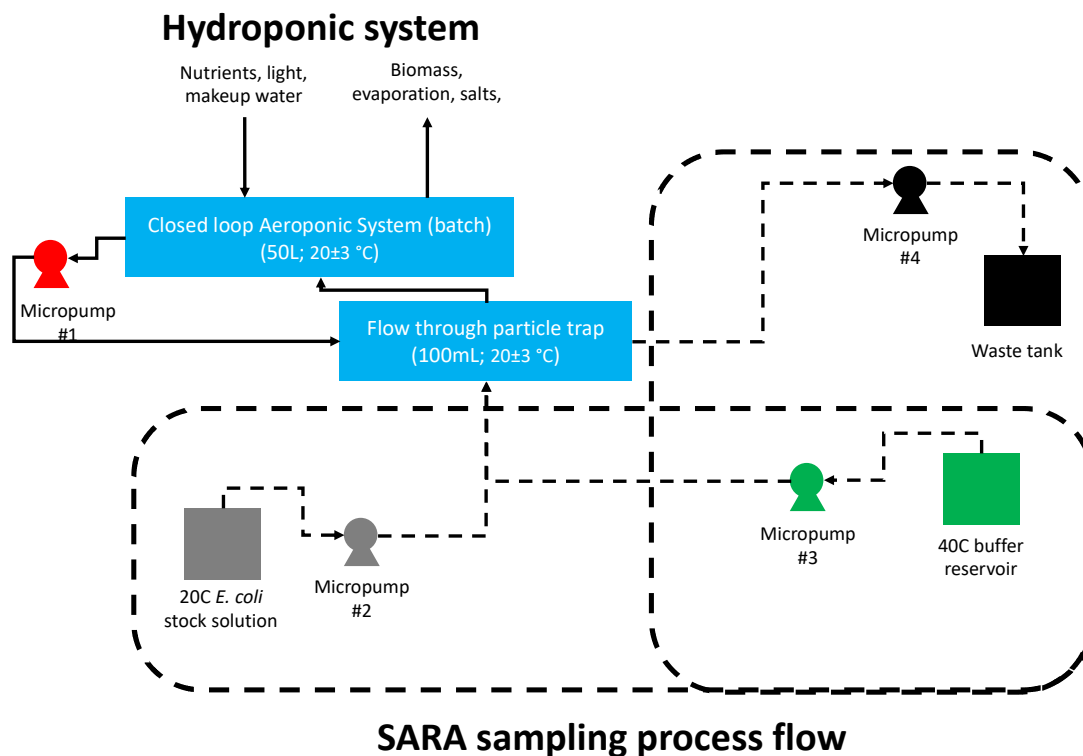
Figure S3. Simplified process flow diagram showing semi-closed loop batch aeroponic system and SARA biosensor loop. The SARA loop contained 3 microcontroller-operated pumps, a stock solution of *E. coli* at 20 ± 1 °C, a PBS buffer at 40 ± 1 °C and a waste tank.

(1) Stop pump #1

↓

(2) Start pump #2, run for 5 min

↓

(3) Impedance measurement

↓

(4) Start pump #3, run for 5 min

↓

(5) Wait 5 min

↓

(6) Impedance measurement

↓

(7) Data analysis

↓

(8) Start pump #4 (to waste)
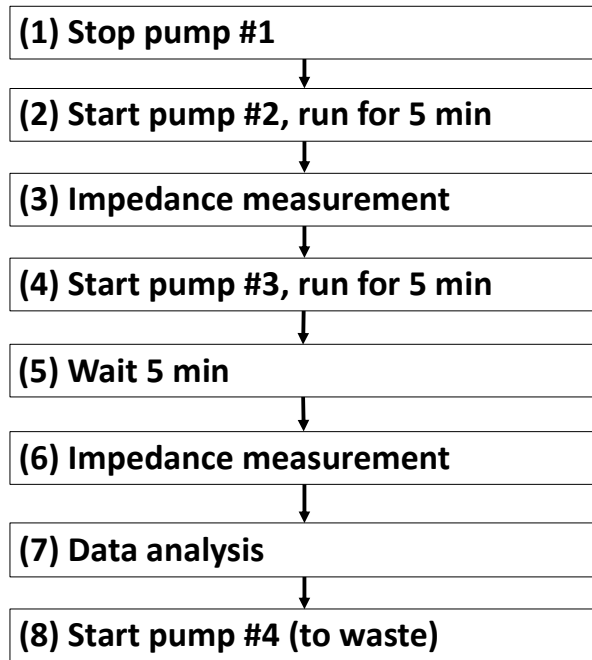
Figure S4. SARA workflow for programming the microcontroller. After stopping the sample pump and adding a known amount of *E. coli*, an electrochemical test was triggered by the program. These steps are summarized as: stop pump #1, then wait 2 sec; start pump #2 for 5 min, then wait 5 min; start pump #3 for 5 min, then wait 5 min; initiate biosensor impedance measurement; then data analysis; start pump #4; initiate decision support program. In total, the sequence required approximately 40 min. Code available upon request.

SARA decision tree
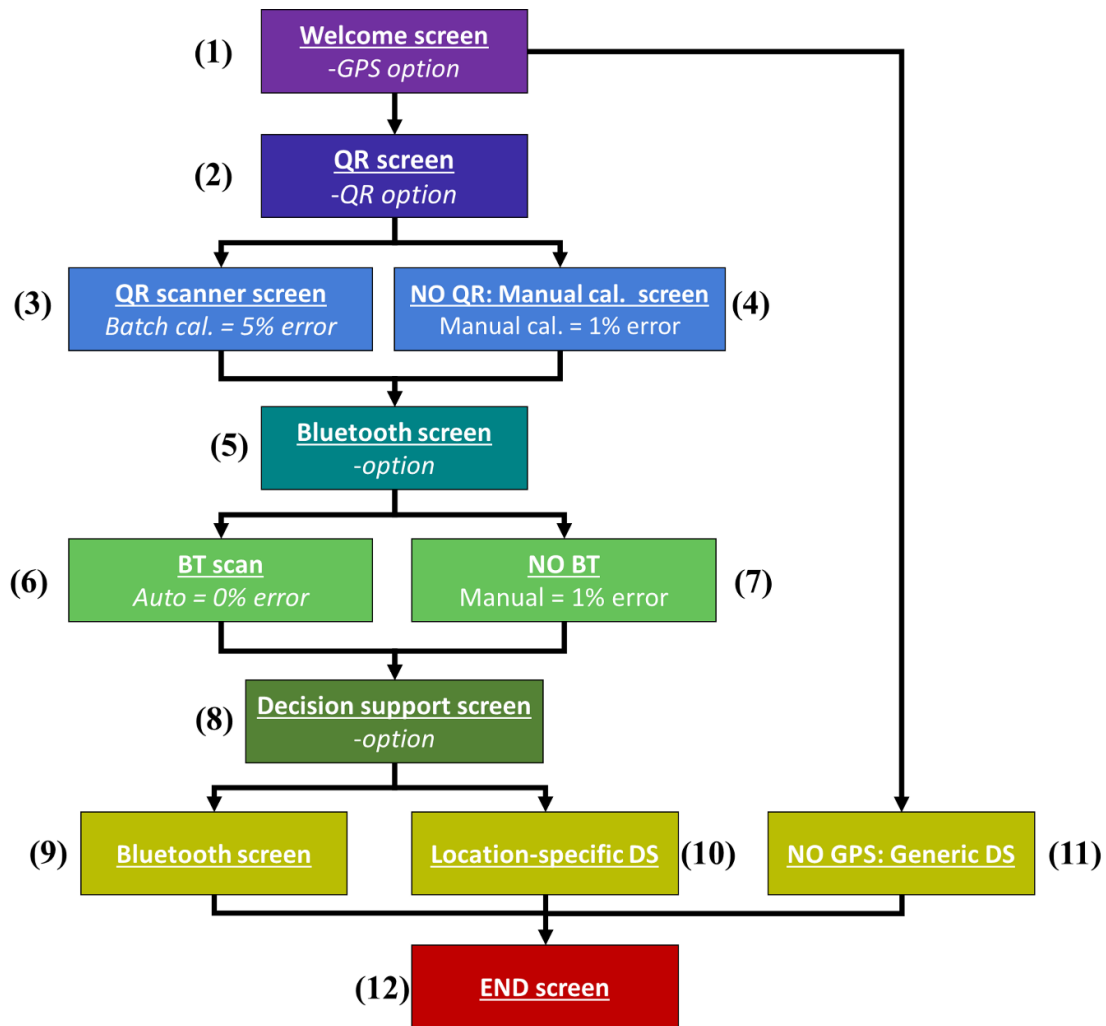
Figure S5. Decision tree for the design of decision support application of SARA. The design includes 12 main screens with four decision points and multiple sources of propagated error. The end results contain multiple sources of propagated error which are estimated using data from sensor testing results (e.g., batch calibration error) or user error (e.g., manual calibration/data entry).

Program

The original code for ShotBot is available at: https://www.instructables.com/id/ShotBot-Arduino-Powered-Pump-Project/. The original code for AirPiano is available at: https://drive.google.com/file/d/1-E0i1CWxxHpTxtieTizCmZC6Bq6q8Tlc/view.

Biofunctionalization

For the attachment of ConA or anti-GroEL antibody to nPt-rGO modified electrodes, the surface was initially carboxylated with a self-assembly monolayer (SAM) using 11-MUA, followed by amine-carboxyl conjugation chemistry. Briefly, electrodes were immersed in 11-MUA solution (150 nM in ethanol) for 30 min at room temperature[2,3]. Next, electrodes were rinsed with RO water, immersed in a EDC/NHS solution (4 mg EDC and 6 mg NHS for 10 mL MES buffer), and agitated for 50 min at room temperature to allow for the activation of SAM[2,4,5]. Electrodes were then immersed in ConA and anti-GroEL antibody suspensions at either 50 nM, 100 nM, or 200 nM concentrations in 10 mM PBS, pH 7.4 and allowed to react for 2 h with agitation at room temperature[5,6]. In order to promote carbohydrate binding and achieve optimum ConA activity, 1 mM Ca^{2+} and 1 mM Mn^{2+} ions were added to the PBS solution[3,7,8].

SEM nPt-rGO electrodes with PNIPAAm
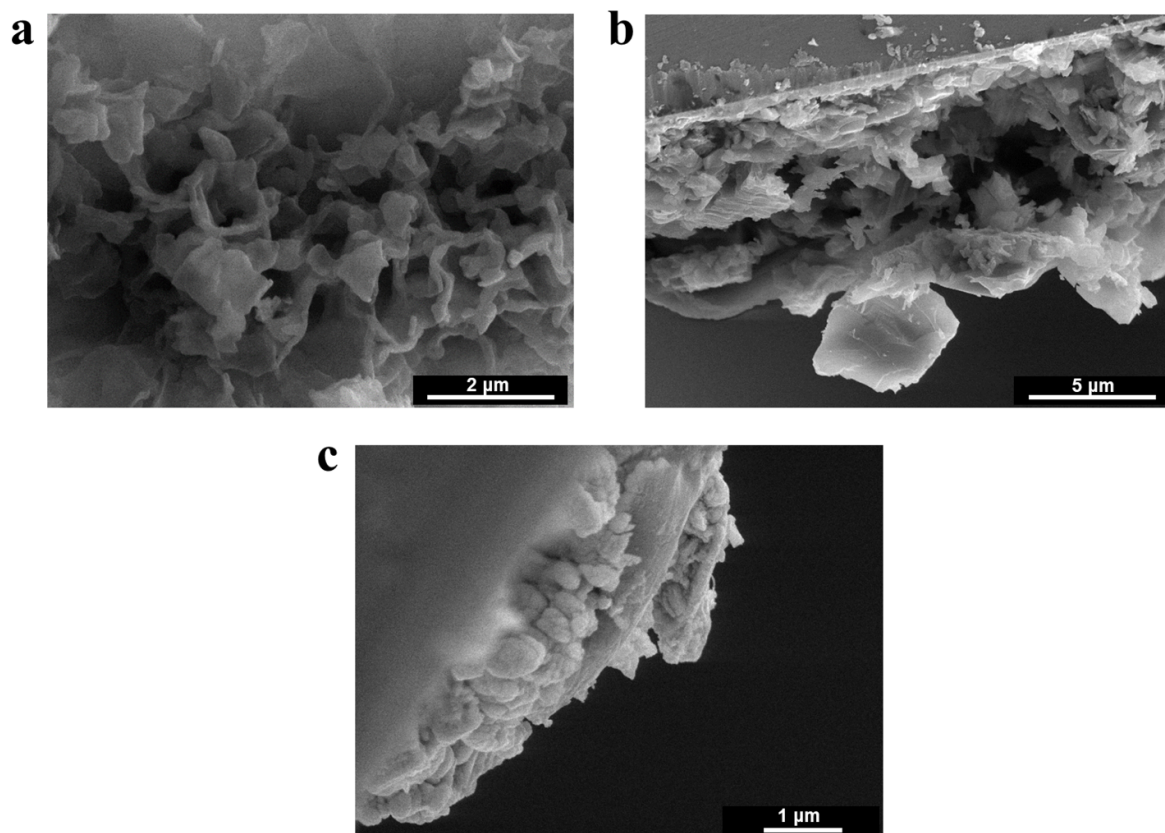
Figure S6. SEM images of nPt-rGO electrodes with PNIPAAM nanobrushes. (**a**) top view and (**b-c**) cross-sectional view at 10 kV and 25,000, 10,000, and 29,000 times magnification, respectively.

PNIPAAm loading

For the electrodes modified with PNIPAAm and functionalized with *E. coli* antibodies (Figure S7 a and b), the ones loaded with 100 nM presented the highest ESA value ($p < 0.05$) not being significantly different from the ones with 50 nM. No difference ($p > 0.05$) was observed when electrodes with and without PNIPAAm nanobrush loaded with 100 nM of antibody were compared. Additionally, oxidation/reduction peaks for 100 nM antibody loading were higher than those observed for other concentrations tested. Moreover, based on Figure S7 b, it seems that above 100 nM loading the electrodes have reached a saturation point.

For ConA, nPt-rGO-PNIPAAm-modified electrodes presented similar ($p > 0.05$) ESA independent of the concentration loaded (Figure S7 c and d). Based on the behavior of the ESA results (Figure S7 d), it is also possible to assume that above 100 nM loading the electrodes have reached a saturation point. The influence of the nanobrushes on the ESA for using the same ConA loading (100 nM) was also evaluated. The presence of PNIPAAm significantly reduced ($p < 0.05$) the ESA of the electrodes. ConA deposition onto nPt-rGO-modified electrodes was achieved through the use of 11-MUA SAM's, while glutaraldehyde and AESH were used to initiate ConA attachment to nPt-rGO-PNIPAAm-modified electrodes. This difference in methods for ConA attachment likely contributes to the differences in ESA observed for ConA loading. Furthermore, covalent crosslinking between the biosensor platform of the non-conductive material of ConA and PNIPAAm was expected to negatively affect the resulting ESA[9].

Considering the highest values of ESA observed for both recognition agents (antibody and ConA) and the loading saturation indicated in Figures S7b and d, 100 nM was, therefore, chosen as the loading concentration to be used for further testing with nPt-rGO-PNIPAAm-modified electrodes.
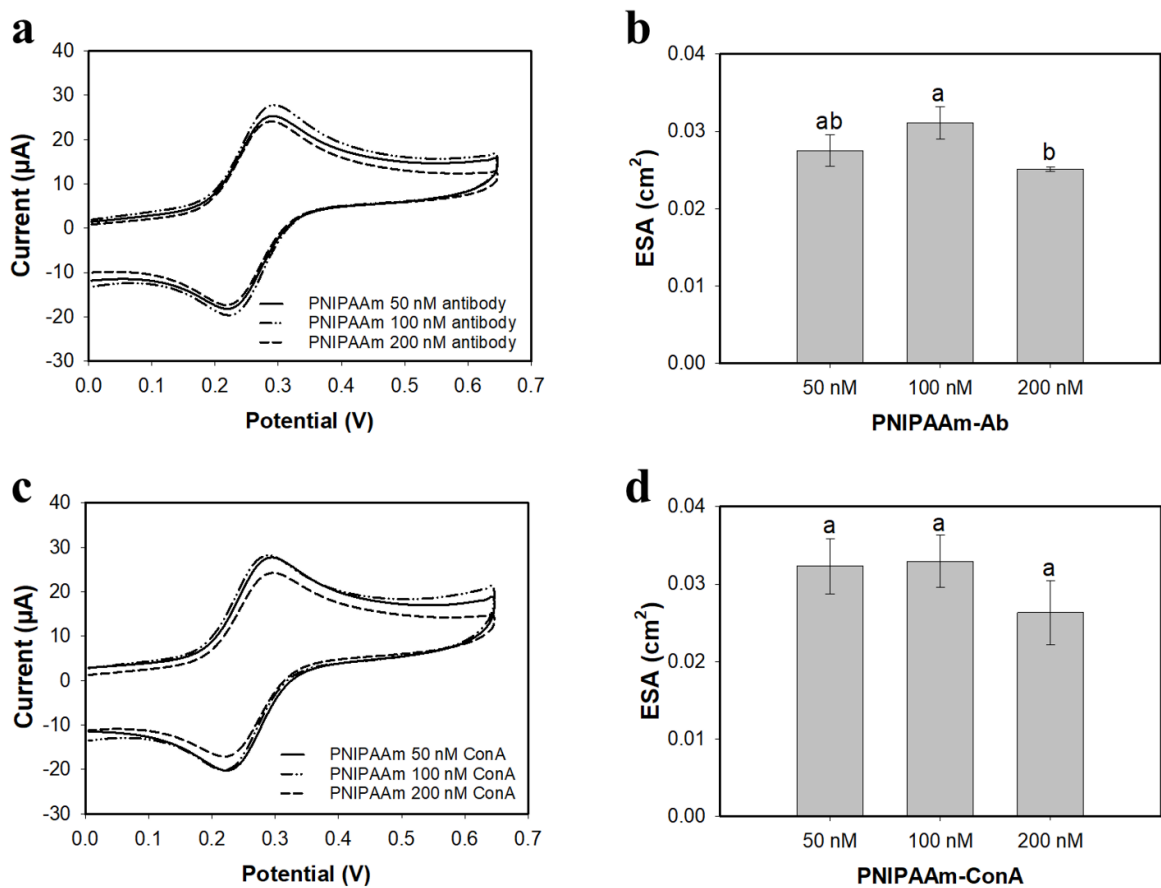
Figure S7. Representative CV curves at 100 mV s^{-1} and comparison of ESA in cm^2 for nPt-rGO-PNIPAAm-modified electrodes at different (**a**, **b**) antibody concentration; and (**c**, **d**) ConA concentrations. Curves represent the average of 3 replications. Bars denoted by different letters are significantly different from each other ($p < 0.05$). Error bars represent the standard deviation.

Nanobrush sensing in buffer

Nyquist plot for ConA-coated nanobrush sensors targeting *E. coli* K12 (Figure S8 a) and *E. coli* K12 in the presence of *Salmonella* Enteritidis (Figure S8 b) in PBS were obtained with an AC amplitude of 0.1 V and initial DC potential of 0.25 V over a frequency range of 1-100,000 Hz.
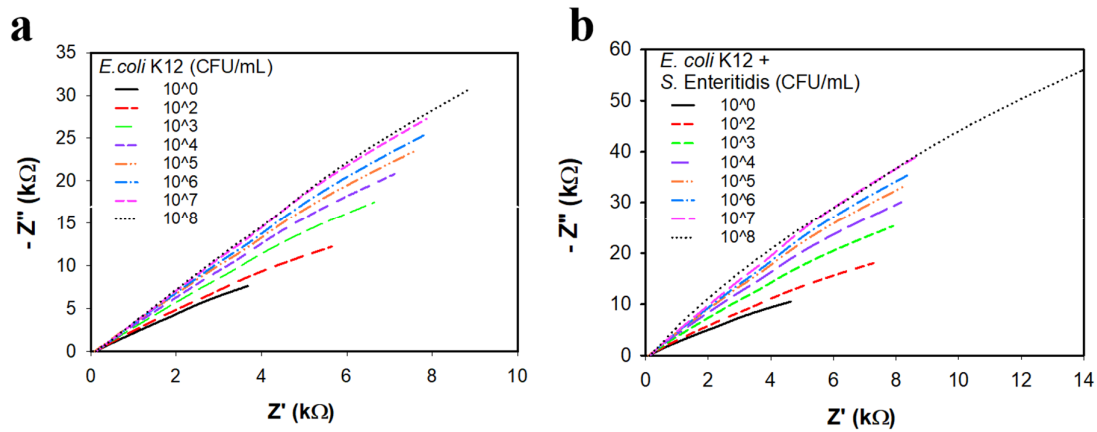
Figure S8. Representative Nyquist plots for PNIPAAm brush sensors decorated with ConA over the frequency range of 1-100,000 Hz exposed to (**a**) *E. coli* K12 (CFU/mL), and (**b**) equal concentrations of *E. coli* K12 and *Salmonella* Enteritidis (CFU/mL) in PBS.

Nanobrush sensing in food samples

Nyquist plot for ConA-coated (Figure S9 a) and Anti-GroEL (Figure S9 b) nanobrush sensors in the presence of bacteria concentrations varying from 10-10^8 CFU/mL in vegetable broth were obtained with an AC amplitude of 0.1 V and initial DC potential of 0.25 V was applied over a frequency range of 1-100,000 Hz.
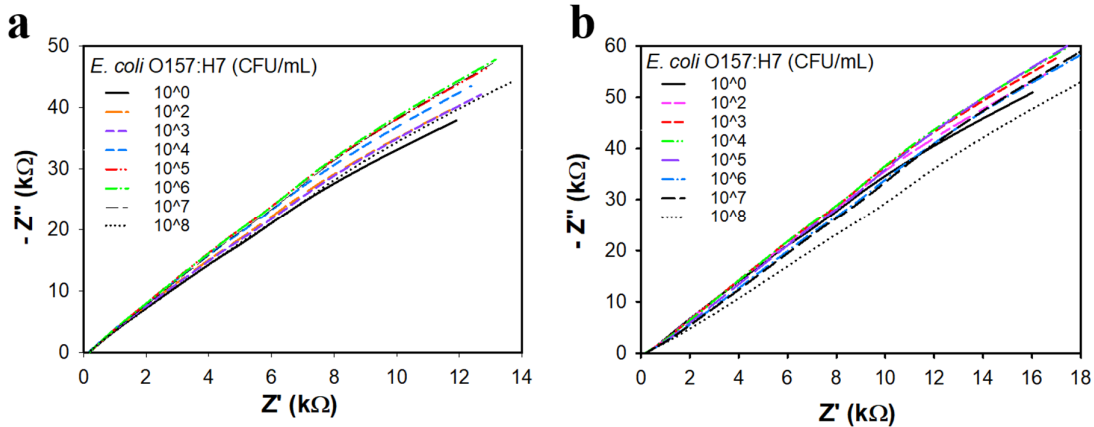
Figure S9. Representative Nyquist plots over the frequency range of 1-100,00 Hz for PNIPAAm brush sensors decorated with (**a**) ConA; and (**b**) Anti-GroEL antibody exposed to various concentrations of *E. coli* O157:H7 (CFU/mL) in vegetable broth.

E. coli sensing in buffer

Electrochemical impedance spectroscopy (EIS) was used to measure the electrochemical response produced by nPt-rGO-ConA and nPt-rGO-Anti-GroEL antibody biosensors when exposed to *E. coli* K12 at concentrations varying from 10^2 - 10^7 CFU/mL without the presence of PNIPAAm nanobrushes. All tests were performed in PBS at a neutral pH with bacteria capture taking place at 20 °C and sensing at 40 °C. As for all the electrodes tested, the time required for bacteria capture was 15 min and EIS measurement required 2 min to run for a total capture and testing time of 17 min. Figures S10 a and b show Bode plots for nPt-rGO-ConA and nPt-rGO-AntiGroEL sensors, respectively, which relates the imaginary portion of the impedance response, -Z″ (Ω), over a frequency range of 1-100,000 Hz for varying bacteria concentrations in PBS. The insets of the figure are an exploded view of the frequency (1 Hz) for each corresponding biorecognition agent that produced the best linear range over the bacteria concentrations tested. EIS data displayed in the form of Nyquist plots is also shown in Figure S10 (c and d), relating the real portion of impedance, Z′ (Ω), to the imaginary portion, -Z″ (Ω) with the frequency increasing from right to left on the plot. Figures S10 e shows the linear portion of the calibration curves for both electrodes with exposure to *E. coli* K12. Calibration curves were created using data obtained at 1 Hz. The calibration curves show the relationship between the bacteria concentration tested (CFU/mL) and the change in the total impedance, Z (%), observed.
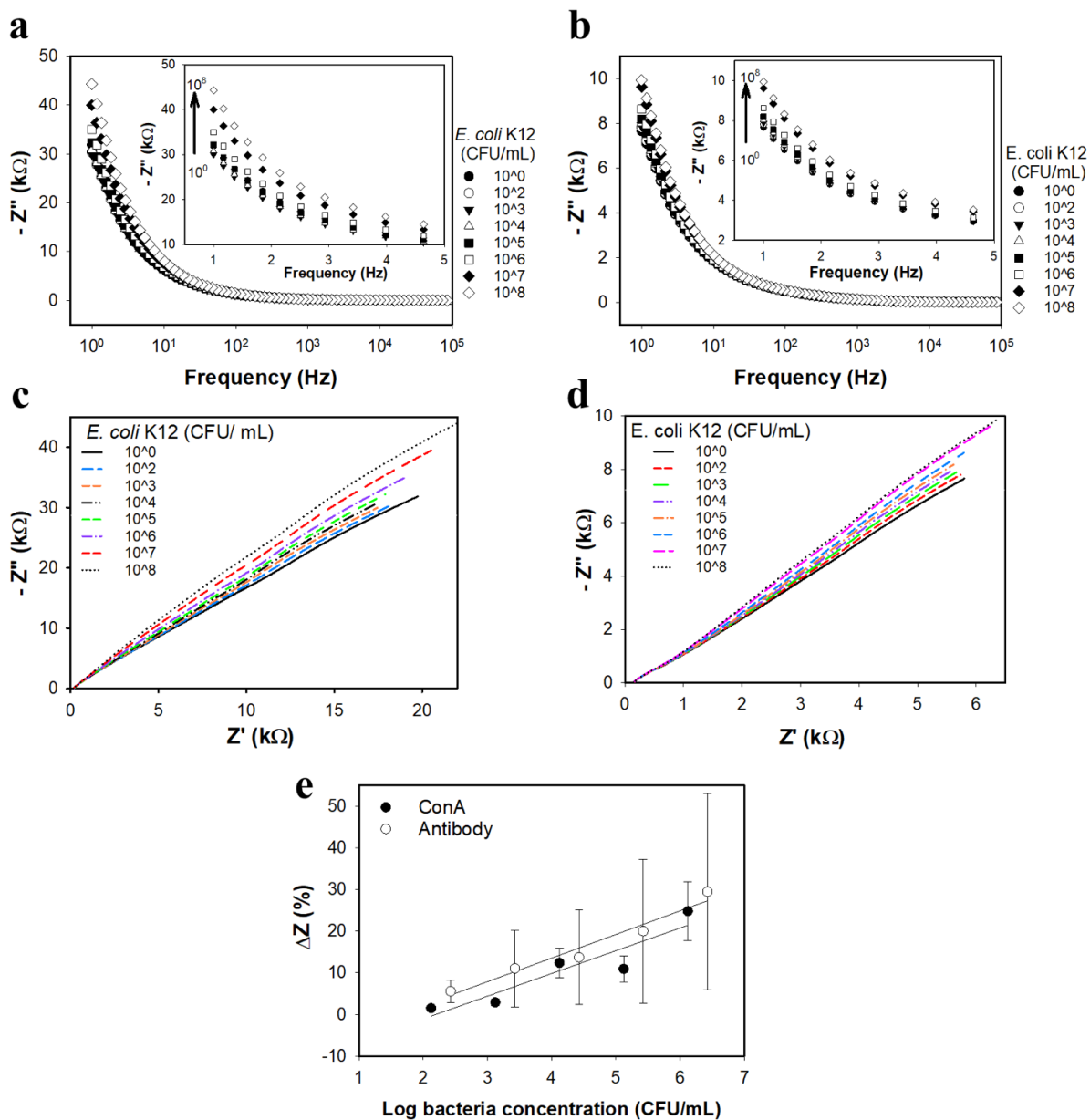
Figure S10. Representative Bode plots over the frequency range of 1-100,000 Hz for (**a**) nPt-rGO-ConA and (**b**) nPt-rGO-Anti-GroEL antibody modified electrodes exposed to various concentrations of *E. coli* K12 (CFU/mL) in PBS. Insets show the exploded view over the frequency range of 1-5 Hz. Representative Nyquist plots for (**c**) nPt-rGO-ConA modified electrodes and (**d**) nPt-rGO-Anti-GroEL antibody modified electrodes exposed to various concentration of *E. coli* K12 (CFU/mL) in PBS. (**e**) calibration curves at 1 Hz for nPt-rGO-ConA and nPt-rGO-Anti-GroEL antibody modified electrodes exposed to *E. coli* K12 in PBS over their respective linear ranges. All data represents the average of 3 repetitions. Error bars represent standard deviation.

Range and lower limit of detection (LOD) were determined from the linear regions of the calibration curves for nPt-rGO-ConA and nPt-rGO-Anti-GroEL sensors. The LOD for the nPt-rGO-Anti-GroEL antibody (732.4 ± 292.9 CFU/mL) was significantly smaller ($p < 0.05$) than the nPt-rGO-ConA (16133.4 ± 8873.6 CFU/mL), which is expected due to the high specificity and bind affinity intrinsic to antibodies[10]. The sensitivity (slope of the calibration curves on Figure S10 e) of nPt-rGO-ConA sensor (559.4 ± 310.1 Ω/log(CFU/mL)) was similar ($p > 0.05$) to nPt-rGO-Anti-GroEL antibody sensor (287.9 ± 120.9 Ω/log(CFU/mL)) for *E. coli* K12, indicating that both are potential recognition agents for the detection of *E. coli* K12. Despite of the difference in LOD, ConA was selected for further testing with the PNIPAAm nanobrushes, considering the similar sensitivity value, its significantly lower cost and extended shelf-life compared to the antibody[11].

The significantly lower LOD ($p < 0.05$) and higher sensitivities ($p < 0.05$) obtained when the electrodes were coated with the PNIPAAm nanobrushes (main article) indicates that the use nPt-rGO-PNIPAAm is crucial for a better performance of the *E. coli* sensor, when compared to nPt-rGO alone.

In initial trials, nanobrushes were functionalized with receptor proteins, either Concanavalin A (Con A) or an antibody (Anti-GroEL, group 1 chaperonin), and two types of linkers were tested. In buffer and broth solutions, ConA sensors had the same selectivity toward *E. coli* O157:H7 as Anti-GroEL sensors, which was further explored by testing affinity toward *Salmonella* Enteritidis (see main manuscript).

SARA: Sense-Analyze-Respond-actuate
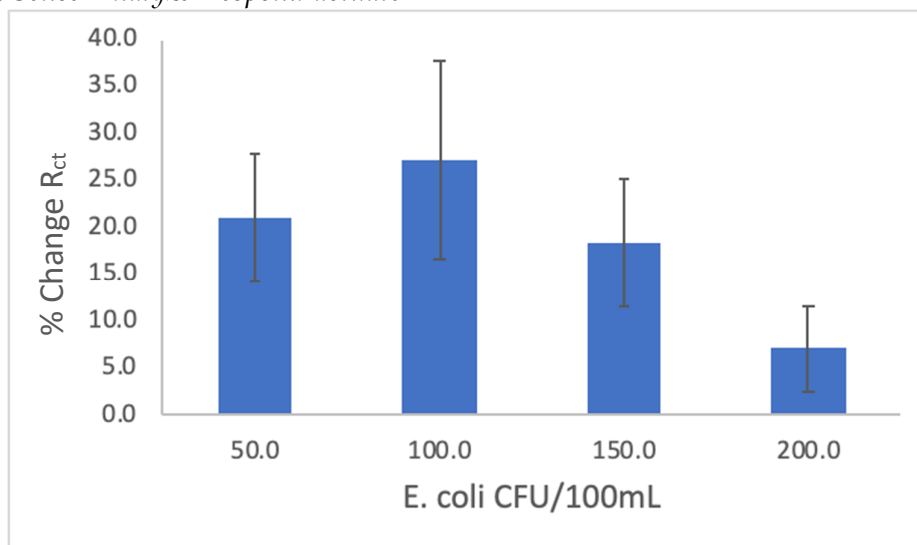
Figure S11. Percent change in R_{ct} during SARA system testing. The percent change decreased significantly with increasing *E. coli* concentration.

References

1. Soares, R.R.A.; Hjort, R.G.; Pola, C.C.; Parate, K.; Reis, E.L.; Soares, N.F.F.; McLamore, E.S.; Claussen, J.C.; Gomes, C.L. Laser-Induced Graphene Electrochemical Immunosensors for Rapid and Label-Free Monitoring of Salmonella enterica in Chicken Broth. *ACS Sensors* **2020**, *5*, 1900-1911, doi:10.1021/acssensors.9b02345.

2. Jantra, J.; Kanatharana, P.; Asawatreratanakul, P.; Hedström, M.; Mattiasson, B.; Thavarungkul, P. Real-time label-free affinity biosensors for enumeration of total bacteria based on immobilized concanavalin A. *Journal of Environmental Science and Health, Part A* **2011**, *46*, 1450-1460, doi:10.1080/10934529.2011.609022.

3. Safina, G.; van Lier, M.; Danielsson, B. Flow-injection assay of the pathogenic bacteria using lectin-based quartz crystal microbalance biosensor. *Talanta* **2008**, *77*, 468-472, doi:https://doi.org/10.1016/j.talanta.2008.03.033.

4. Campuzano, S.; Orozco, J.; Kagan, D.; Guix, M.; Gao, W.; Sattayasamitsathit, S.; Claussen, J.C.; Merkoçi, A.; Wang, J. Bacterial Isolation by Lectin-Modified Microengines. *Nano Letters* **2012**, *12*, 396-401, doi:10.1021/nl203717q.

5. Hermanson, G.T. Chapter 4 - Zero-Length Crosslinkers. In *Bioconjugate Techniques (Third Edition)*, Hermanson, G.T., Ed. Academic Press: Boston, 2013; https://doi.org/10.1016/B978-0-12-382239-0.00004-2pp. 259-273.

6. Hu, Y.; Zuo, P.; Ye, B.-C. Label-free electrochemical impedance spectroscopy biosensor for direct detection of cancer cells based on the interaction between carbohydrate and lectin. *Biosensors and Bioelectronics* **2013**, *43*, 79-83, doi:https://doi.org/10.1016/j.bios.2012.11.028.

7. Gamella, M.; Campuzano, S.; Parrado, C.; Reviejo, A.J.; Pingarrón, J.M. Microorganisms recognition and quantification by lectin adsorptive affinity impedance. *Talanta* **2009**, *78*, 1303-1309, doi:https://doi.org/10.1016/j.talanta.2009.01.059.

8. Lu, Q.; Lin, H.; Ge, S.; Luo, S.; Cai, Q.; Grimes, C.A. Wireless, remote-query, and high sensitivity Escherichia coli O157:H7 biosensor based on the recognition action of concanavalin A. *Analytical chemistry* **2009**, *81*, 5846-5850, doi:10.1021/ac9008572.

9. Burrs, S.L.; Vanegas, D.C.; Bhargava, M.; Mechulan, N.; Hendershot, P.; Yamaguchi, H.; Gomes, C.; McLamore, E.S. A comparative study of graphene–hydrogel hybrid bionanocomposites for biosensing. *Analyst* **2015**, *140*, 1466-1476, doi:10.1039/C4AN01788A.

10. Cesewski, E.; Johnson, B.N. Electrochemical biosensors for pathogen detection. *Biosensors and Bioelectronics* **2020**, *159*, 112214, doi:https://doi.org/10.1016/j.bios.2020.112214.

11. Liu, X.; Ou, X.; Lu, Q.; Chen, S.; Wei, S. A biorecognition system for concanavalin a using a glassy carbon electrode modified with silver nanoparticles, dextran and glucose oxidase. *Microchimica Acta* **2015**, *182*, 797-803, doi:10.1007/s00604-014-1390-7.